Zeeman splitting of double-donor spin-triplet levels in silicon

R. E. Peale, K. Muro,* and A. J. Sievers
Laboratory of Atomic and Solid State Physics, Cornell University, Ithaca, New York 14853-2501

F. S. Ham
Department of Physics and Sherman Fairchild Laboratory, Lehigh University, Bethlehem, Pennsylvania 18015
(Received 23 December 1987)

Observation of the Zeeman effect has confirmed the identification of spin-triplet terms for double donors in silicon. The isotropic splitting of an absorption line at 2146.38 cm^{-1} in Si:Se^0, and of the corresponding line at 1218.37 cm^{-1} in Si:Te^0, into two σ components and one π component is consistent with their identification with the $\mathcal{J}=1$ spin-orbit level of the $1s(A_1)1s(T_2)$ configuration's $^3T_2$ spin-triplet term. An experimental splitting factor $g_{\mathcal{J}}$ of this line equal to 1.0 for both systems agrees with the theory of Landé g factors when the orbital g factor g_L equals zero as predicted by effective-mass theory. The spin-orbit interaction parameter determined from a nonlinear component in the Zeeman splitting predicts a ratio of singlet and triplet absorption strengths which agrees with the observed ratio to within a factor of 2 for Si:Te^0 but only to within a factor of 3 for Si:Se^0.

I. INTRODUCTION

Since a double donor in silicon is a solid-state analog of the helium atom, spin-triplet terms should exist among the donor's excited states in addition to the spin-singlet terms commonly observed in ir spectra.[1,2] The energy difference between triplet and singlet terms of the same two-electron configuration being a consequence of Coulomb repulsion between electrons, we expect this separation to be larger the more compact the electronic wave function. In terms of effective-mass theory, which has been used successfully in describing the states of the substitutional double donors S^0, Se^0, and Te^0 in silicon,[1,2] we accordingly expect this separation to be most easily resolved in the $1s(A_1)1s(T_2)$ configuration, in which one electron has been raised from its $1s(A_1)$ ground state to its lowest excited, valley-orbit-split state $1s(T_2)$. In recent experiments Bergman *et al.*[3] have shown that uniaxial stress causes a new ir-absorption line to appear in the spectrum of Si:Se^0, and they have identified this line with the transition to a stress-split component of the $^3T_2$ term of the $1s(A_1)1s(T_2)$ configuration. According to this interpretation, which is consistent with Hund's rules, the energy of the $^3T_2$ term in zero stress lies ~ 50 cm^{-1} below that of $^1T_2$, in an energy region in which no spin-singlet states should exist. A similar feature[3] for Si:Te^0 corresponds to a line at ~ 1218 cm^{-1} in the zero-stress spectrum that had previously been attributed to an oxygen impurity.[4] Spin-orbit interaction provides the coupling of the spin-singlet and spin-triplet terms that relaxes the usual spin selection rule $\Delta S=0$ in the optical spectrum.

Stress does not lift the spin degeneracy of a level, however, so the work of Bergman *et al.*[3] does not directly demonstrate the threefold spin multiplicity of the new state they have observed. The purpose of this paper is to test their identification of this new line with the $^3T_2$ term by confirming this multiplicity from the splitting of this line in a magnetic field. Our preliminary high-resolution spectroscopic survey[5,6] showed that this forbidden transition could be observed in zero stress for Si:Se^0 as well as for Si:Te^0. Because of the magnetic moment associated with electron spin, we expect this line to show a linear Zeeman effect with three components. Moreover, according to effective-mass theory the orbital magnetic moment of the $1s(A_1)1s(T_2)$ configuration is zero, and the $g_{\mathcal{J}}$ factor describing the splitting of the observed line should therefore have a value close to unity, as will be shown. Our experimental confirmation of this prediction not only confirms the identification of Bergman *et al.*[3] of this line with the spin-triplet state, but also confirms the validity of effective-mass theory in describing the magnetic behavior of this state. We have also been able to infer the strength of the spin-orbit interaction from a quadratic component in the Zeeman splitting, and we have measured directly the singlet-triplet energy separation and the ratio of singlet and triplet line strengths. These results are compared with the independent determination of the spin-orbit interaction strength from the stress measurements of Bergman *et al.*[3]

Section II develops the theory of the spin-orbit and Zeeman splitting of the $^3T_2$ term of the $1s(A_1)1s(T_2)$ configuration using the analogy of a ^3P term of a free atom and the formalism of the theory of the Landé g factor. The spin-orbit mixing of the $^3T_2$ and $^1T_2$ terms is related to the one-electron spin-orbit–coupling parameter ξ used by Bergman *et al.*,[3] and the effect of this mixing on the energy levels and g factor is given. Section III outlines the experimental details, describes the confirmation of the spin-triplet assignment and the extraction of the $g_{\mathcal{J}}$ factors and spin-orbit–coupling parameters, and compares the measured line-strength ratios with the values

 ©1988 The American Physical Society

predicted by combining our theory both with our own experimentally determined parameters and with those of Bergman *et al.*[3] We discuss our conclusions in Sec. IV.

II. THEORY

A. Symmetry of states; spin-orbit splitting

The ground level of a substitutional double donor in Si in its neutral charge state, as treated in effective-mass theory[7–9] (EMT), has two electrons in the $1s(A_1)$ state, the symmetric combination[9,10] of $1s$ effective-mass states from the six conduction-band valleys, with total spin $S=0$. This $^1A_1$ state belongs to the irreducible representation[11] Γ_1 of the tetrahedral point group (T_d). Optical excitation to the $^1T_2$ level (Γ_5), in which one electron is raised to one of the $1s(T_2)$ states formed by the antisymmetric combinations[9,10] of valleys from the [100], [010], and [001] axes (labeled x, y, and z), is, in principle, allowed through central-cell corrections to EMT. Optical excitation to the corresponding $^3T_2$ level with $S=1$ requires, in addition, the presence of spin-orbit interaction[3] to relax the spin selection rule $\Delta S=0$ through mixing with $^1T_2$. This $^3T_2$ term has spin-orbit components transforming as Γ_2, Γ_3, Γ_4, and Γ_5, and it is only the Γ_5 component that has the same symmetry as $^1T_2$ and can mix with it. In full tetrahedral symmetry, optical excitation from $^1A_1$ is therefore possible only to the Γ_5 component of $^3T_2$.

Within the $^3T_2$ term, the spin-orbit interaction takes the simple form

$$\mathcal{H}_{\text{s.o.}}=\lambda(\mathcal{L}\cdot\mathbf{S}) , \tag{1}$$

as in a ^3P term of a free atom, where λ is the spin-orbit–coupling parameter for the $^3T_2$ term. In Eq. (1), $\mathcal{L}$ is an effective orbital angular momentum[12] with components $\mathcal{L}_x,\mathcal{L}_y,\mathcal{L}_z$ defined to have matrix elements with respect to the two-electron orbital T_2 states T_{2x},T_{2y},T_{2z} identical to those that the true orbital angular momentum $\mathcal{L}$ has with respect to atomic P state P_x,P_y,P_z,

$$\langle T_{2y}\,|\,\mathcal{L}_x\,|\,T_{2z}\rangle=\langle P_y\,|\,L_x\,|\,P_z\rangle=-i, \quad \cdots \tag{2}$$

$\mathcal{L}_x,\mathcal{L}_y,\mathcal{L}_z$ satisfy the commutation rules for an angular momentum, and from Eq. (2) we have $\mathcal{L}=1$. Introducing an effective total angular momentum $\mathcal{J}=\mathcal{L}+\mathbf{S}$, we find, as in the Landé interval rule for the relative energies of the spin-orbit levels of a ^3P term, that we have three levels with $\mathcal{J}=0$, 1, and 2 and energies -2λ, $-\lambda$, and $+\lambda$, respectively. These levels belong to the irreducible representations Γ_2, Γ_5, and $\Gamma_3+\Gamma_4$, respectively. The spin-orbit splittings are depicted in the energy-level diagram shown in Fig. 1.

B. Zeeman effect

The linear Zeeman coupling of a $^3T_2$ state with a magnetic field $\mathbf{B}$ may be written as

$$\mathcal{H}_Z=g_{\mathcal{L}}\mu_B\mathcal{L}\cdot\mathbf{B}+g_S\mu_B\mathbf{S}\cdot\mathbf{B} , \tag{3}$$

where μ_B is the Bohr magneton and $g_{\mathcal{L}}$ and g_S are orbital and spin g factors. Within a level of given $\mathcal{J}$, matrix elements of $\mathcal{H}_Z$ from Eq. (3) are equal to those of the operator

$$\mathcal{H}_Z(\mathcal{J})=g_{\mathcal{J}}\mu_B\mathcal{J}\cdot\mathbf{B} , \tag{4}$$

as in the theory[13] of the Landé g factor, with $g_{\mathcal{J}}$ given for both $\mathcal{J}=1$ and 2 of $^3T_2$ by

$$g_{\mathcal{J}}=(g_{\mathcal{L}}+g_S)/2 . \tag{5}$$

We can expect $g_S=2$ to sufficient accuracy, since spin-resonance studies[10,14] of shallow single donors in Si show only a slight departure from the free-electron spin-only value, while measurements[4] for the singly ionized donors Se^+ and Te^+ yield values of 2.0057 and 2.0023, respectively. To evaluate $g_{\mathcal{L}}$ we equate a representative matrix element of the first term in Eq. (3) to the corresponding matrix element of the interaction of the orbital magnetic moments of the individual electrons with the magnetic field,

$$g_{\mathcal{L}}\mu_B\langle T_{2y}\,|\,\mathcal{L}_x\,|\,T_{2z}\rangle = \frac{e}{2mc}\left\langle T_{2y}\left|\sum_{n=1,2}(\mathbf{r}_n\times\mathbf{p}_n)_x\right|T_{2z}\right\rangle , \tag{6}$$

where $\mathbf{r}_n$ and $\mathbf{p}_n$ denote the coordinate and momentum operators of the nth electron. The left-hand side of Eq. (6) equals $-ig_{\mathcal{L}}\mu_B$ from Eq. (2), but in the effective-mass approximation the right-hand side is zero because the ex-

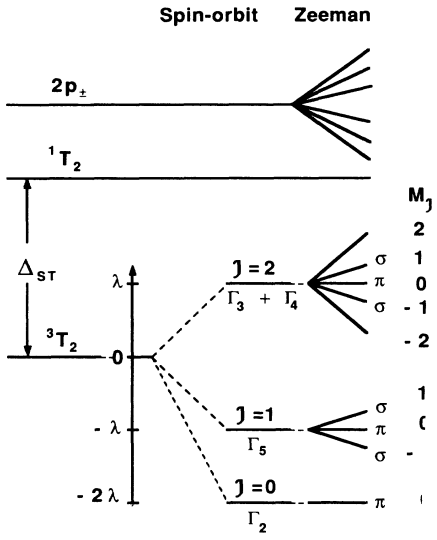

FIG. 1. Schematic, silicon-double-donor, energy-level diagram identifying the triplet levels. This energy-level diagram shows the relative energies of the $^3T_2$, $^1T_2$, and $2p_\pm$ irabsorption lines and the effects of the spin-orbit and Zeeman interactions for an arbitrary sample orientation in the magnetic field. Also shown for the spin-orbit levels of the $^3T_2$ term are the irreducible representations by which they transform and the values of effective total angular momentum. The observed polarization and the component of the effective total angular momentum along the magnetic field for each Zeeman component are indicated. The energies are not to scale.

cited electron in the state T_{2y} or T_{2z} is in the state $1s(T_{2y})$ or $1s(T_{2z})$ formed from valleys on the y and z axes, respectively. Intervalley matrix elements of $\mathbf{r}\times\mathbf{p}$ can be shown from the work of Luttinger and Kohn[8] to be zero; hence $g_\perp$ equals zero.[15] Corrections to the effective-mass approximation, leading to a nonzero value for $g_\perp$, are, of course, necessary if central-cell corrections cause the $1s(T_2)$ state to involve, for example, significant admixtures of p functions on the donor impurity. From a value $g_\perp \approx 0$, we may accordingly expect, from Eq. (5), $g_\mathcal{J} \approx 1$ for the Zeeman splitting of both levels $\Gamma_5(\mathcal{J}=1)$ and $\Gamma_3+\Gamma_4(\mathcal{J}=2)$, the former being the only level that should be observed in the optical excitation spectrum at fields low enough that mixing of states of different $\mathcal{J}$ is not significant.

At higher fields, mixing between states of different $\mathcal{J}$ increases, and energy levels depend nonlinearly on B. In addition, optical excitation becomes possible to those states of the $\mathcal{J}=0,2$ levels which mix with those of $\mathcal{J}=1$. However, $\mathcal{H}_Z$ in Eq. (3) is still diagonal with respect to the component of $\mathcal{J}$ along the field, and states with different eigenvalues $M_\mathcal{J}=0,\pm1,\pm2$ with respect to this component of $\mathcal{J}$ do not mix (so long as the Γ_3 and Γ_4 components of $\mathcal{J}=2$ are not separated by higher-order effects). The Zeeman splitting is then isotropic. The relative energies of the two states with $M_\mathcal{J}=+1$ are given exactly (except in omitting the effect of spin-orbit coupling between $^3T_2$ and $^1T_2$) by

$$E_{+1}=\tfrac{1}{2}(g_S+g_\perp)\mu_B B\pm[\lambda^2+\tfrac{1}{4}(g_S-g_\perp)^2(\mu_B B)^2]^{1/2}\ , \tag{7}$$

and those for $M_\mathcal{J}=-1$ by

$$E_{-1}=-\tfrac{1}{2}(g_S+g_\perp)\mu_B B\pm[\lambda^2+\tfrac{1}{4}(g_S-g_\perp)^2(\mu_B B)^2]^{1/2}\ . \tag{8}$$

The lower sign in both Eqs. (7) and (8) corresponds to the states originating in the $\Gamma_5(\mathcal{J}=1)$ level. States with $M_\mathcal{J}=0$ are given by the three roots of the equation

$$E^3+2\lambda E^2-[\lambda^2+(g_S-g_\perp)^2(\mu_B B)^2]E-2\lambda^3=0\ , \tag{9}$$

of which the one originating in $\mathcal{J}=1$ is found from Eq. (9) to be approximated by

$$E_0=-\lambda(1-\tfrac{1}{2}\alpha^2+\tfrac{3}{8}\alpha^4-\tfrac{7}{16}\alpha^6+\cdots)\ , \tag{10}$$

with $\alpha=(g_S-g_\perp)(\mu_B B/\lambda)$. Finally, states with $M_\mathcal{J}=\pm2$ have energies

$$E_{\pm2}=\lambda\pm(g_S+g_\perp)\mu_B B\ . \tag{11}$$

All Zeeman splittings are depicted schematically in Fig. 1.

C. Spin-orbit coupling of $^1T_2$ and $^3T_2$ terms; zero-field oscillator-strength ratio

A calculation of the oscillator-strength ratio $R=f_1/f_3$ corresponding to the $^1A_1\rightarrow{}^1T_2$ and $^1A_1\rightarrow{}^3T_2$ transitions in the absence of magnetic fields or strain has already been given by King and Van Vleck[16] for the equivalent problem of the $^1S\rightarrow{}^1P$ and $^1S\rightarrow{}^3P$ excitations of a free atom such as mercury having the ground-state electronic configuration $(ns)^2$. The same problem has also been considered by Knox and Dexter[17] for the impurity ion Tl^+ in an alkali halide crystal. This calculation[16,17] yields the result

$$R=(\nu_1/\nu_3)(K/\xi)^2\ , \tag{12}$$

where ν_1/ν_3 denotes the ratio of the corresponding transition energies, ξ is the one-electron spin-orbit parameter for the $1s(T_2)$ state, and K is given by

$$K=\sqrt{2}\{(G+\tfrac{1}{4}\xi)+[(G+\tfrac{1}{4}\xi)^2+\tfrac{1}{2}\xi^2]^{1/2}\}\ , \tag{13}$$

Here, G is the exchange integral[13,16] between the $1s(A_1)$ and $1s(T_2)$ orbitals, in terms of which the energy difference[3] Δ_{ST} of the $^3T_2$ and $^1T_2$ terms when spin-orbit coupling vanishes ($\xi=0$) is

$$\Delta_{ST}=2G\ . \tag{14}$$

Spin-orbit coupling between the $^3T_2$ and $^1T_2$ terms modifies the relative energy positions of their spin-orbit levels. In terms of ξ and G these are given exactly in zero magnetic field by

$$E[^3T_2,\Gamma_2]=-G-\xi\ , \tag{15a}$$

$$E[^3T_2,\Gamma_5]=-\tfrac{1}{4}\xi-[(G+\tfrac{1}{4}\xi)^2+\tfrac{1}{2}\xi^2]^{1/2}\ , \tag{15b}$$

$$E[^3T_2,\Gamma_3,\Gamma_4]=-G+\tfrac{1}{2}\xi\ , \tag{15c}$$

$$E[^1T_2,\Gamma_5]=-\tfrac{1}{4}\xi+[(G+\tfrac{1}{4}\xi)^2+\tfrac{1}{2}\xi^2]^{1/2}\ . \tag{16}$$

The relationship of ξ to the spin-orbit parameter λ of the $^3T_2$ term, introduced in Eq. (1), is seen by comparing Eq. (15) with Eqs. (7)–(11), in the limit of weak coupling ($G\gg\xi$), to be

$$\lambda=\xi/2\ . \tag{17}$$

Spin-orbit coupling of the $^3T_2$ and $^1T_2$ terms also modifies the $g_\mathcal{J}$ factor of the Γ_5 ($\mathcal{J}=1$) level of the $^3T_2$ term from that given by Eq. (5). Following King and Van Vleck, we obtain for the exact $g_\mathcal{J}$ factor of this level

$$g_\mathcal{J}=g_\perp+\tfrac{1}{2}(g_S-g_\perp)/[1+(\xi/K)^2]\ . \tag{18}$$

The possibility that spin-orbit coupling between the $^3T_2$ and $^1T_2$ terms might be different from that within $^3T_2$ can be included by adapting the work of King and Van Vleck.[16] Such a difference occurs for free atom ^3P and ^1P terms, these authors noted, because the one-electron np orbitals have somewhat different radial wave functions in the singlet and triplet states. If a similar difference is present in the $1s(T_2)$ orbital of the $^3T_2$ and $^1T_2$ terms of the double donor, the oscillator-strength ratio R, the level positions as given in Eqs. (12)–(16), and the g factor given by Eq. (18) must be modified. Preserving the relationship in Eq. (17) but modifying the spin-orbit interaction between $^3T_2$ and $^1T_2$ to correspond to a coupling parameter $\xi\gamma$, we find from the results of King and Van Vleck that the terms $\xi^2/2$ in Eqs. (13), (15), and (16) must be replaced by $\xi^2\gamma^2/2$, $(K/\xi)^2$ in Eq. (12) by $(K/\xi\gamma)^2$, and $(\xi/K)^2$ in Eq. (18) by $(\xi\gamma/K)^2$.

III. EXPERIMENT DETAILS AND RESULTS

A. Measurements

Our Si:Se^0 samples were prepared by high-temperature diffusion in fused quartz ampoules containing, besides the sample and dopant, half an atmosphere of He gas. The sample used in our Zeeman measurements was cooled slowly in the furnace after the diffusion. The tubes were made as small as possible to avoid sample corrosion due to the vapor-phase transport of material to cooler regions of our globar furnace. Our Te-doped silicon samples were prepared by vapor-phase epitaxy described elsewhere.[4] All spectra were taken with the sample immersed in pumped liquid helium at a temperature of 1.7 K and with the optical-access cryostat, fitted with ZnSe and NaCl windows, placed in the beam of an IBM Fourier-transform infrared interferometer (FTIR). When polarized light was required, either a wire-grid or a Brewster's-angle ZnSe-plate polarizer was placed in the FTIR beam before the cryostat. Magnetic fields were applied by placing the sample in the bore of 4-T solenoid or a 2-T split coil in the same cryostat. The well-known effective-mass-enhanced, highly anisotropic Zeeman splitting of the $2p_{\pm}$ line[18] was used to verify the sample orientation in the field and to accurately determine the field strength. Since no broadening of the split lines was observed even at the highest fields, we conclude that the magnetic fields were homogeneous over the sample region probed by the FTIR beam.

In our Si:Se^0 samples, a weak but sharp line was observed at 2146.38 cm^{-1}, near the expected zero-stress position of the forbidden $^3T_2$ transition inferred by Bergman *et al.*,[3] but too sharp to have been observed in their 1-cm^{-1} resolution zero-stress spectra. Our 0.25-cm^{-1}-resolution ir spectrum reveals a 0.3-cm^{-1} linewidth (full width at half maximum). The nearby $^1T_2$ singlet at 2195.52 cm^{-1} has a 0.5-cm^{-1} width. The singlet-to-triplet integrated absorption-coefficient ratio in eight different diffusion-doped Si:Se^0 samples is 46 ± 10. The triplet line in Si:Te^0 appears at 1218.37 cm^{-1}, and our 0.1-cm^{-1}-resolution spectrum reveals a width of 0.4 cm^{-1} for this line and 2.9 cm^{-1} for the $^1T_2$ line at 1287.73 cm^{-1}. The singlet-to-triplet integrated absorption-coefficient ratio for Si:Te^0 in eight samples is 10 ± 1.

The transmission spectra for both Si:Se^0 and Si:Te^0 appear in Fig. 2. The broad ionization absorption and many sharp absorption lines are visible in the higher-energy region of the spectrum. The excited states of these transitions are hydrogenic owing to the strong screening of the donor nucleus by the electron remaining in the ground state. In Fig. 2 we label only the $2p_{\pm}$ line used in determining the sample orientation and magnetic field strength. The exchange interaction between an electron in one of these hydrogenic orbitals and the electron in the ground orbital is so weak that any difference in energy between singlets and triplets is masked by the linewidths of these transitions, so triplet terms associated with these higher excited states are not seen in absorption. On the other hand, an electron in the $1s(T_2)$ orbital

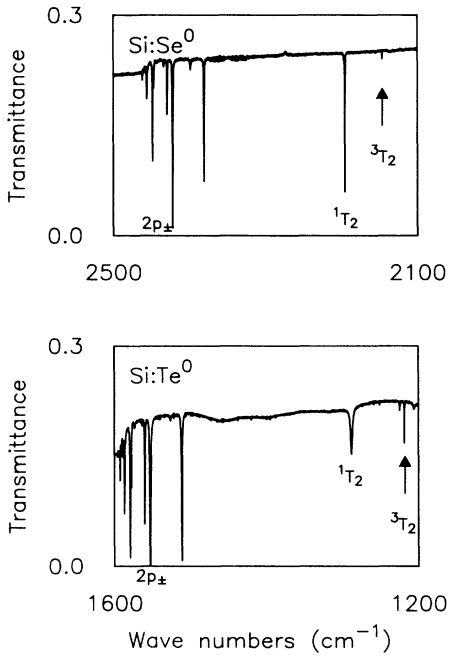

FIG. 2. Si:Se^0 and Si:Te^0 ir-transmission spectra. Transitions to the $^1T_2$ singlet term, the $\delta=1$ spin-orbit level of the $^3T_2$ triplet term, and $2p_{\pm}$ are indicated.

has a relatively large exchange interaction with the ground-state electron, leading to an energy difference which is clearly resolved in the ir spectra, as seen in the lower-energy portion of Fig. 2. The triplet term in each spectrum is indicated by an arrow. The weak line on the low-frequency side of the Te^0 triplet is a vibrational mode of an oxygen-related defect.[19] The weak line on the high-frequency side is not in the right energy region, according to Eq. (11), to be the $\delta=2$ spin-orbit level of the $^3T_2$ term, and it splits in a magnetic field like $np_{\pm}$, indicating that it belongs to the absorption series of an unknown donor.

The Zeeman measurements were performed in the Faraday configuration, using a solenoid, in which the FTIR-beam propagation vector is parallel to the magnetic field, and in the Voigt configuration, using a split coil, in which the propagation vector is perpendicular to the field. Since, in the Faraday configuration, the electric field vector of the incident FTIR beam is perpendicular to the magnetic field for any polarization, only the two σ Zeeman components are observed. In the Voigt configuration, the electric field vector is polarized either parallel or perpendicular to the magnetic field so that either the central π Zeeman component or the σ components can be observed.

One of the triplet line's distinguishing features is the striking difference between its Zeeman splitting and that of transitions to final states, like $2p_{\pm}$, whose orbital magnetic moment is nonzero. The splitting of the $2p_{\pm}$ line is enhanced by the ratio of the free-electron mass to the effective mass and is proportional to the cosine of the angle between the symmetry axes of the conduction-band minima and the magnetic field.[18] Figure 3 compares the

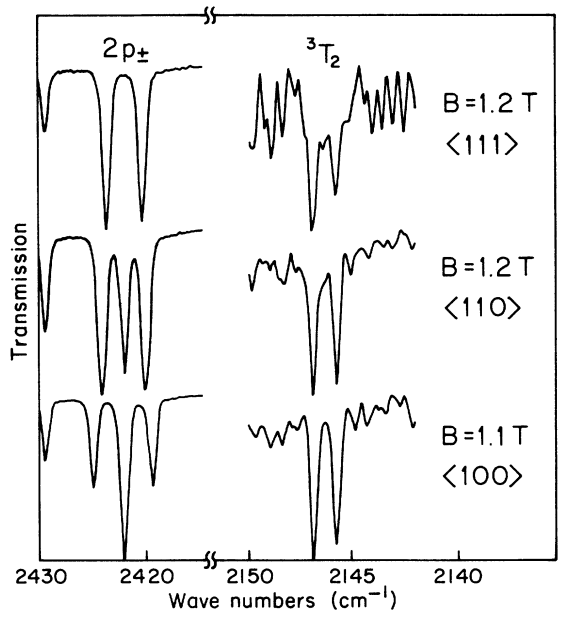

FIG. 3. Zeeman spectra of the Si:Se^0 $2p_\pm$ and $^3T_2(\mathcal{J}=1)$ lines. The isotropic Zeeman splitting of the Si:Se^0 $^3T_2(\mathcal{J}=1)$ line is compared with the effective-mass-enhanced, anisotropic splitting of the $2p_\pm$ line for three sample orientations in a Faraday-configured field of ~ 1 T.

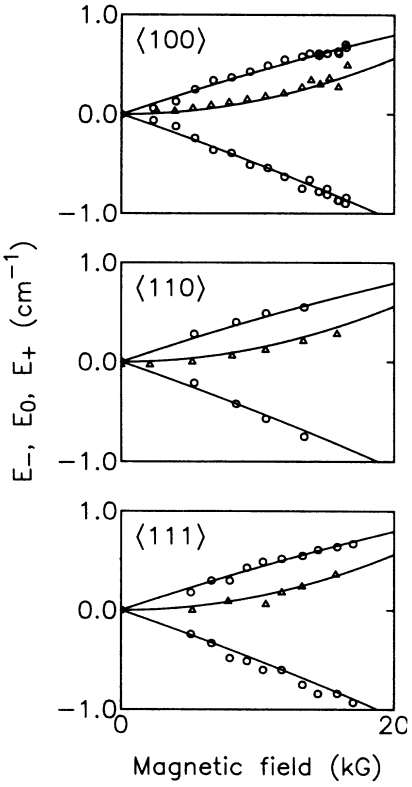

FIG. 4. Demonstration of the isotropy of the Si:Se^0 $^3T_2(\mathcal{J}=1)$ π and σ components. The measured center frequencies vs magnetic field of the π ($\triangle$ data) and σ ($\circ$ data) Zeeman components of the Si:Se^0 $^3T_2(\mathcal{J}=1)$ line for three sample orientations in a Voigt-configured field are plotted. The theoretical curves (solid lines) are the same for each orientation.

Zeeman splittings of the $2p_\pm$ and $^3T_2(\mathcal{J}=1)$ lines for three orientations of the Si:Se^0 sample in a 1-T Faraday-configured field. The $2p_\pm$ splitting is large and highly anisotropic in both pattern and magnitude, but the triplet splitting is small and isotropic. The line on the high-frequency side of $2p_\pm$ is $3p_0$, which is not split in a magnetic field.

Figure 4 shows the measured center frequencies versus magnetic field of the π and σ Zeeman components of the Si:Se^0 $^3T_2(\mathcal{J}=1)$ line for sample oriented with $\langle 100\rangle$, $\langle 110\rangle$, and $\langle 111\rangle$ axes along the magnetic field. For each orientation, we plot the theoretical curves for $E_\pm$ from Eqs. (7) and (8) and E_0 from Eq. (10), setting $g_\perp = 0$ and using the experimentally determined spin-orbit parameter discussed below and given in Table I. It is evident that the σ components lie on the $E_\pm$ curves and that the π component lies on the E_0 curve for all three sample orientations. This provides the strongest evidence for the isotropy of the splitting.

The corresponding plot for the Si:Te^0 triplet is shown in Fig. 5 for a sample oriented with its $\langle 100\rangle$ axis along the magnetic field vector. Once again, the theoretical curves, with the experimentally determined spin-orbit parameter and with $g_\perp = 0$, match the data closely. It was not possible to study other orientations owing to the wafer sample geometry.

The center frequencies versus magnetic field of the $^3T_2(\mathcal{J}=1)$ spin-triplet σ Zeeman components for both Si:Se^0 and Si:Te^0 systems in a Faraday-configured field are plotted in Fig. 6. We also plot the theoretical curves $E_\pm$ from Eqs. (7) and (8), with $g_\perp = 0$ and with the experimentally determined spin-orbit parameter extracted from the data below and appearing in Table I. For our cubic Si:Se sample, both $\langle 100\rangle$ and $\langle 110\rangle$ orientations in the magnetic field were possible. The two data sets are superimposed here, and the good overlap further demonstrates the isotropy of the splitting. The Si:Te^0 data were all taken with the $\langle 100\rangle$ sample axis parallel to the field, and

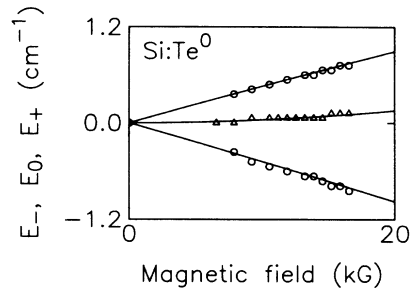

FIG. 5. Zeeman splitting of the Si:Te^0 $^3T_2(\mathcal{J}=1)$ line in a Voigt-configured field. The center frequencies vs magnetic field of both π ($\triangle$ data) and σ ($\circ$ data) components with the field oriented along a $\langle 100\rangle$ axis are plotted along with the theory (solid line).

TABLE I. Double-donor parameters. The values, from the stress [Bergman *et al.* (Ref. 3)] and Zeeman experiments (present work) are compared. The parameters are the frequencies of the $^1T_2$ and $^3T_2$ lines, the spin-orbit interaction coefficient λ determined from the σ components of the Faraday data, the spin-orbit interaction coefficient λ_π determined from the π component of the Voigt data, the one-electron spin-orbit parameter ξ, the measured singlet-triplet energy separation Δ, this separation when spin-orbit interaction vanishes, Δ_{ST}, the predicted ratio of $^1T_2$ and $^3T_2$ line strengths, R_t, the measured values R_e, and the triplet $\mathcal{J}=1$ level's $g_{\mathcal{J}}$ values.

	Present work		Bergman *et al.*[a]	
	Se^0	Te^0	Se^0	Te^0
ν_1 (cm^{-1})	2195.52	1287.73		
ν_3 (cm^{-1})	2146.38	1218.37	~2145	1217
λ (cm^{-1})	3.1±0.1	11.1±0.3		
λ_π (cm^{-1})	3.0	8.4		
ξ (cm^{-1})	6.2	22.2	3.2	12.4
Δ (cm^{-1})	49.14	69.36		
$\Delta_{ST}(=2G)$ (cm^{-1})	45.2±0.1	50.7±0.3	48.5	65.5
R_t	126	18	470	60
R_e	46±10	10±1		
$g_{\mathcal{J}}(\mathcal{J}=1)$	1.01±0.01	0.990±0.004		

[a]Reference 3.

data taken at both 0.5- and at 0.1-cm^{-1} resolution are plotted together. Note that the Te^0 splitting is more nearly linear than the Se^0 splitting owing to its larger spin-orbit interaction parameter and hence larger separation of spin-orbit components.

B. Parameter identification

We obtain the spectroscopic splitting factor $g_{\mathcal{J}}$ from the linear part of the Zeeman effect by fitting $E_{+1}-E_{-1}$ versus magnetic field, using the Faraday data and the difference of Eqs. (7) and (8). In Fig. 7 the linear fits are plotted as solid lines with the data for both systems. From the linearity of the data it is evident that manipulation of the data in this way does indeed cancel the quadratic part of the effect. According to our theory, the slope of the fit should equal $2g_{\mathcal{J}}\mu_B$ for the $\mathcal{J}=1$ component of the $^3T_2$ term. For this component these data yield $g_{\mathcal{J}}$ values of 1.01±0.01 (Se^0) and 0.990±0.004 (Te^0).

The spin-orbit interaction parameter is determined from the second-order part of the Zeeman effect by fitting $-(E_{+1}+E_{-1})$ versus B^2, using the Faraday data and the binomial expansion of the sum of Eqs. (7) and (8), in which $g_{\mathcal{L}}$ is taken to be zero. In Fig. 8 the linear fits are plotted as solid lines through the data points for both sys-

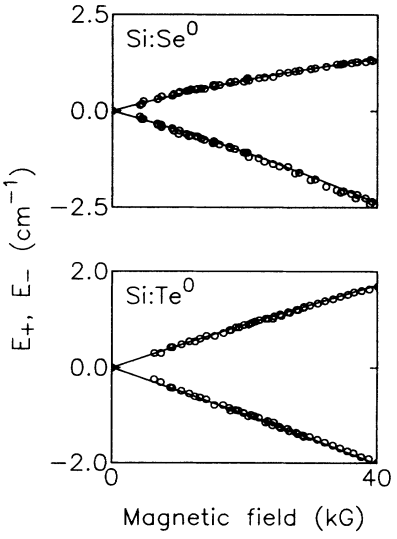

FIG. 6. Zeeman splitting of the $Si:Se^0$ and $Si:Te^0$ $^3T_2(\mathcal{J}=1)$ lines in Faraday-configured field. Theory curves are plotted as solid lines.

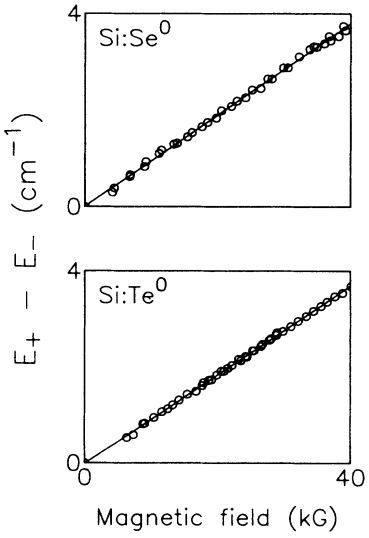

FIG. 7. Linear fit of $E_{+1}-E_{-1}$ vs magnetic field. The difference between the E_{+1} and E_{-1} components of the $^3T_2(\mathcal{J}=1)$ line from the $Si:Se^0$ and $Si:Te^0$ Faraday data is represented by the open circles and the fit is plotted as a solid line.

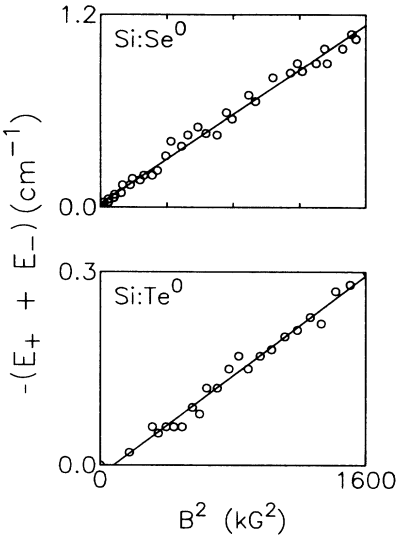

FIG. 8. Linear fit of $-(E_{+1}+E_{-1})$ vs the square of the magnetic field. The sum of the E_{+1} and E_{-1} components of the $^3T_2(\mathcal{J}=1)$ line from the Si:Se^0 and Si:Te^0 Faraday data is represented by the open circles and the fit is plotted as a solid line.

tems. Only the highest-resolution data for Si:Te^0 are used here, for it can be seen that the second-order effect is small for this system. The linearity of the points demonstrates that manipulation of the data in this way allows one to focus exclusively on the quadratic part of the splitting. According to our theory, the slope of the fit should be $(\mu_B^2)/\lambda$; hence λ is 3.1 ± 0.1 cm^{-1} for Se^0 and 11.1 ± 0.3 cm^{-1} for Te^0. The stress measurements of Bergman *et al.*[3] provide values for the parameter ξ, which we determined from Eq. (17) and our values for λ. The comparisons are made in Table I.

The measured energy difference Δ between the singlet and triplet lines is equal to the difference between Eqs. (16) and (15b). Since we now know ξ, the exchange integral G can be extracted from Δ. Inserting G into Eq. (14) gives the singlet-triplet energy difference Δ_{ST} in the absence of spin-orbit coupling. Since this last parameter is one determined in the stress experiments of Bergman *et al.*,[3] we have obtained a second parameter by which to compare the Zeeman and stress methods. This comparison is made in Table I, in which both Δ and Δ_{ST} are given.

Both ξ and G are used in Eq. (13) to find the parameter K, which is needed in Eq. (12) for the singlet-to-triplet oscillator-strength ratio. We find that these ratios are 126 ± 6 for Se^0 and 18 ± 1 for Te^0. These values are to be compared with the measured ratios 46 ± 10 (Se) and 10 ± 1 (Te). The predicted and measured oscillator-strength ratio values are included in Table I, where they are compared with the values obtained by using the results of Bergman *et al.*[3] in our theory.

An alternative determination of the spin-orbit interaction parameter, which we distinguish by adding the subscript π to the symbol λ, is provided by fitting the π-component data to Eq. (10) for E_0. The coefficient of the second-order term for the Se^0 π data is found to be 1.4×10^{-3} cm^{-1}/kG^2, which gives $\lambda_\pi=3.0$ cm^{-1}. For the Te^0 data, the coefficient of the second-order term is 5.2×10^{-4} cm^{-1}/kG^2, which gives $\lambda_\pi=8.4$. These λ_π values appear in Table I. The λ_π are not as precise as the λ values, found from the fit of the Faraday-data σ components, for there are fewer π data points and they do not extend as far in field.

IV. CONCLUSIONS AND DISCUSSION

Our initial purpose was to confirm, from their Zeeman splitting, that the new line in the ir spectrum of Si:Se^0 and the corresponding line in Si:Te^0 result from a transition into a double-donor spin-triplet level, as concluded by Bergman *et al.*[3] This line is indeed split by a magnetic field into three components, but for both Si:Se^0 and Si:Te^0 its isotropic $g_{\mathcal{J}}$ factor has the value 1, far from the value 2 expected for a transition into a level with simple spin degeneracy. However, the $^3T_2$ term of the excited $1s(A_1)1s(T_2)$ configuration has triple orbital degeneracy in addition to its threefold spin degeneracy. If, as a result of central-cell corrections to EMT, spin-orbit splitting of $^3T_2$ is large compared with the Zeeman splitting, only transitions to the triply degenerate $\Gamma_5(\mathcal{J}=1)$ spin-orbit level should be observed, and the $g_{\mathcal{J}}$ factor of this level is predicted to be unity if there is no contribution to the magnetic coupling from the orbital magnetic moment. This vanishing of the orbital moment is exactly the prediction of EMT, and we take the observed behavior as confirmation not only of the identification of the new line by Bergman *et al.*[3] with the $^3T_2$ term but also of the accuracy of EMT in describing the magnetic behavior of this state. Though the $\mathcal{J}=0$ and 2 spin-orbit levels of the $^3T_2$ term were not directly observed, the magnetic coupling between them and the $\mathcal{J}=1$ level has been related to the nonlinear part of the Zeeman splitting of the $\mathcal{J}=1$ level, and this behavior has been used to determine the value of the spin-orbit splitting.

Although there must be a significant central-cell correction to EMT for both Si:Se^0 and Si:Te^0 to account for the large spin-orbit splitting of the $^3T_2$ term, this correction must still be too small to cause a significant departure of the $g_{\mathcal{J}}$ factor from the value of 1. This is reasonable, since the one-electron spin-orbit parameter[20] for atomic Se in the $4p$ state is of order 1500 or 3000 cm^{-1} in the $5p$ state of Te. Thus a p-function admixture on the central donor atom of order 0.5% would account for the spin-orbit coupling of the $1s(T_2)$ state while giving the orbital g factor g_L a value of order only ~0.005, too small according to Eq. (5) to affect the observed $g_{\mathcal{J}}$ by more than the estimated experimental error.

If there were a significant orbital contribution to the $g_{\mathcal{J}}$ factor, moreover, this coupling should show up directly as a Zeeman splitting of the $^1T_2$ term, which has only orbital degeneracy. No Zeeman splitting of the line corresponding to the $^1A_1\rightarrow{}^1T_2$ transition was observed within our experimental linewidth.

Our determination of the spin-orbit–coupling strength from the quadratic component of the Zeeman energy has

ignored the possibility that these states might show an intrinsic diamagnetism because of their large spatial extent. Such a contribution to the term in the energy quadratic in the field would be positive for all three Zeeman components, however, whereas the quadratic term given by Eqs. (7) and (8) for the $M_J=\pm 1$ states is negative (λ being positive, as found[21] also for Se^+ and Te^+, so that the level with $J=2$ lies at a higher energy than that with $J=1$). The quadratic term for the $M_J=0$ state as given by Eq. (10), on the other hand, is positive. Thus a significant diamagnetic correction to these energies would have led us to obtain different values for λ from the different Zeeman components. The approximate agreement of the value of λ and the value of λ_π thus obtained for each double donor suggests that any diamagnetic shift is not significant. Such a shift would also affect the $^1T_2$ term.

The values for λ obtained in this work correspond to a spin-orbit interaction approximately twice as strong as that inferred by Bergman *et al.*[3] from the form of the avoided crossing of the strain-split components of the $^1T_2$ and $^3T_2$ terms. We could account for this difference in the manner of King and Van Vleck[16] by introducing a factor $\gamma \sim \frac{1}{2}$ in the interterm spin-orbit coupling, as discussed in Sec. II C. As these authors have shown, a value for γ in the range 0.75–0.85 serves quite well to describe the spectra of the free atoms Hg, Cd, Zn, Ba, Sr, and Ca and corresponds to the *np* orbital in the ^1P term being more diffuse than that in the more tightly bound ^3P term. Similarly, we would anticipate a value $\gamma < 1$ for the double donors if the $1s(T_2)$ wave function in the $^1T_2$ term is more extended than in $^3T_2$ and has a smaller central-cell correction. However, use of a value $\gamma \sim \frac{1}{2}$ in Eq. (12) as modified to include γ (Sec. II C) increases the predicted value for the oscillator-strength ratio by a factor ~ 4 and makes worse the approximate agreement exhibited in Table I with the experimental value of this ratio. We have no explanation at present for the difference in the strength of the spin-orbit coupling inferred in our work and in that of Bergman *et al.*[3]

We may, nevertheless, note that the value for the spin-orbit parameter ξ obtained in our work remains smaller than that inferred from the observed[21] spin-orbit splitting of the Γ_7 and Γ_8 components of the $1s(T_2)$ state of the ionized donors $Si:Se^+$ and $Si:Te^+$ ($\xi \sim 12$ and 29 cm^{-1}, respectively). Because the single electron "sees" a doubly charged core in this latter case and is therefore much more tightly bound than for the neutral donor, this case should provide an upper bound for the value of the one-electron spin-orbit coupling of the double donor. So large a value for ξ as that obtained in our work, however, implies, from Eq. (18) (with $g_\perp = 0$), a reduction in the g factor g_J for $J=1$ (to ~ 0.99 for Se and ~ 0.95 for Te) that is in disagreement with the experimental value by more than our limits of uncertainty. A better understanding of the proper value to take for the spin-orbit coupling will probably have to await the direct observation of the spin-orbit levels with $J=0$ and 2 by using higher magnetic fields than those available to us in the present work.

We have already noted in Sec. II C that the $^1T_2$ and $^3T_2$ terms of the double donor exhibit properties analogous to those of the ^1P and ^3P terms of the impurity ion Tl^+ in an alkali halide crystal.[17] Other such mercury-like (or helium-like) defects with the ground-state electronic configuration $(ns)^2$ that have been studied extensively[22] include such ions as Ga^+, In^+, Sn^{2+}, and Pb^{2+} in the alkali halides and the F center[23–25] in CaO. All these defects differ from the double donors in Si, however, in that the *np* electron has a strong Jahn-Teller coupling that dominates spin-orbit coupling. The optical transitions are accordingly broadened into bands, and the Zeeman splitting of the excited states, as studied for example for the F center in CaO by optically detected magnetic resonance,[24,25] is that of a simple spin ($S=1$) in an axially distorted center with g factor near 2 (in actuality a superposition of the spectra of such distorted centers with all crystallographically equivalent orientations). By contrast, the large spatial extent of the effective-mass states of the double donor restricts their Jahn-Teller coupling to phonons of wavelength longer than the orbit diameter, of which there are too few for the Jahn-Teller effect to be significant in comparison with the spin-orbit splitting.[10] The resulting Zeeman splitting is that of the spin-orbit levels in a fully symmetrical environment and is accordingly isotropic, as found in the present work. The double donors, despite their close resemblance to the other mercury-like defect centers, thus represent a very different case more closely resembling the free Hg atom,[16] except in having no contribution to the Zeeman splitting from the orbital magnetic moment.

With the identification of double-donor triplet terms now confirmed, the question of producing a nonequilibrium population in these states arises. Optically pumped double-donor electrons could become trapped in triplet excited states if their lifetimes relative to the singlets are long enough, causing a change in the triplet line strength. We attempted this experiment by irradiating a low-temperature sample with xenon arc light. Spectral changes were easily observed that may be explained by a combination of the Burstein-Moss shift[26,27] and by line narrowing due to screening by photogenerated carriers of the random fields of ionized impurities, but no change in the ratio of the $^1T_2$-to-$^3T_2$ integrated absorption coefficients was detected. These results are consistent with homogeneous broadening of deep-donor absorption lines[28,29] since then the observed small difference between singlet and triplet linewidths illustrated in Fig. 2 would translate into a small difference in singlet and triplet lifetimes, compatible with our null result.

In summary, the identification of spin-triplet terms for double donors in silicon, first detected by Bergman *et al.*,[3] has been confirmed by means of the Zeeman effect. The isotropic Zeeman splitting of the new line in $Si:Se^0$ and of the corresponding line in $Si:Te^0$ into three components having the expected polarizations is consistent with their identification as the $J=1$ spin-orbit level of the $^3T_2$ spin-triplet term of the double-donor $1s(A_1)1s(T_2)$ electronic configuration. The experimental splitting factor $g_J=1$ for both $Si:Se^0$ and $Si:Te^0$ agrees well with the simple theory of Landé g factors using the

EMT value $g_{\perp}=0$. The values of the spin-orbit interaction parameter determined from the fit of the Zeeman data to the theory yield better agreement than those of Bergman *et al.*[3] with the observed ratios of singlet-to-triplet zero-stress transition intensities.

ACKNOWLEDGMENTS

We thank Dr. Peter Wagner and Dr. C. Holm of Heliotronic GmbH for kindly providing us with the tellerium-doped silicon samples used in this research. The work by three of us (R.E.P., K.M., and A.J.S.) was supported by the U.S. National Science Foundation under Grant No. DMR-84-03597 and by the U.S. Army Research Office under Grant No. DAAL03-86-K0103. The portion of this research contributed by F.S.H. was supported by the U.S. Office of Naval Research (Electronics and Solid State Science Program) under Contract No. N00014-84K-0025.

---

*Permanent address: Osaka University, Faculty of Engineering Science, Toyonaka, Osaka, Japan.

[1]E. Janzén, R. Stedman, G. Grossmann, and H. G. Grimmeiss, Phys. Rev. B **29**, 1907 (1984).

[2]P. Wagner, C. Holm, E. Sirtl, R. Oeder, and W. Zulehner, in *Festkörperprobleme,* edited by P. Grosse (Vieweg, Braunschweig, 1984), Vol. 24, p. 191.

[3]K. Bergman, G. Grossmann, H. G. Grimmeiss, and Michael Stavola, Phys. Rev. Lett. **56**, 2827 (1986).

[4]H. G. Grimmeiss, E. Janzén, H. Ennen, O. Schirmer, J. Schneider, R. Wörner, C. Holm, E. Sirtl, and P. Wagner, Phys. Rev. B **24**, 4571 (1981).

[5]R. E. Peale, K. Muro, and A. J. Sievers, Bull. Am. Phys. Soc. **32**, 404 (1987).

[6]R. E. Peale, K. Muro, A. J. Sievers, and F. S. Ham, J. Opt. Soc. Am. A **4**, P65 (1987).

[7]C. Kittel and A. H. Mitchell, Phys. Rev. **96**, 1488 (1954).

[8]J. M. Luttinger and W. Kohn, Phys. Rev. **97**, 869 (1955).

[9]W. Kohn, in *Solid State Physics,* edited by F. Seitz and D. Turnbull (Academic, New York, 1957), Vol. 5, p. 257.

[10]G. D. Watkins and F. S. Ham, Phys. Rev. B **1**, 4071 (1970).

[11]The Mulliken notation A_1, A_2, E, T_1, T_2 [R.S. Mulliken, Phys. Rev. **43**, 279 (1933)] is used to denote the irreducible representations of the symmetry group T_d of the tetrahedron for orbital states, and the Bethe notation $\Gamma_1, \Gamma_2, \Gamma_3, \Gamma_4, \Gamma_5$ [H. A. Bethe, Ann. Phys. (Leipzig) **3**, 133 (1929)] for spin-orbit states.

[12]A. Abragam and M. H. L. Pryce, Proc. R. Soc. London, Ser. A **205**, 135 (1951).

[13]E. U. Condon and G. H. Shortley, *Theory of Atomic Spectra* (Cambridge University Press, Cambridge, 1959).

[14]D. K. Wilson and G. Feher, Phys. Rev. **124**, 1068 (1961).

[15]P. J. Dean, R. A. Faulkner, and S. Kimura, Phys. Rev. B **2**, 4062 (1970).

[16]G. W. King and J. H. Van Vleck, Phys. Rev. **56**, 464 (1939).

[17]R. S. Knox and D. L. Dexter, Phys. Rev. **104**, 1245 (1956).

[18]R. R. Haering, Can. J. Phys. **36**, 1161 (1958).

[19]D. R. Bosomworth, W. Hayes, A. R. L. Spray, and G. D. Watkins, Proc. R. Soc. London, Ser. A **317**, 133 (1970).

[20]C. E. Moore, *Atomic Energy Levels,* Nat. Bur. Stand. (U.S.) Circ. No. 467 (U.S. GPO, Washington, D.C., 1952), Vol. II; *ibid.,* Vol. III (1958).

[21]H. G. Grimmeiss, E. Janzén, and K. Larsson, Phys. Rev. B **25**, 2627 (1982).

[22]Work on the mercury-like ions in alkali halides has been reviewed by V. V. Hizhnyakov and N. N. Kristoffel, in *The Dynamical Jahn-Teller Effect in Localized Systems,* edited by Yu. E. Perlin and M. Wagner (North-Holland, New York, 1984), p. 383.

[23]B. Henderson, S. E. Stokowski, and T. C. Ensign, Phys. Rev. **183**, 826 (1969).

[24]P. Edel, C. Hennies, Y. Merle d'Aubigné, R. Romestain, and Y. Twarowski, Phys. Rev. Lett. **28**, 1268 (1972).

[25]Le Si Dang, Y. Merle d'Aubigné, and Y. Rasoloarison, J. Phys. (Paris) **39**, 760 (1978).

[26]E. Burstein, Phys. Rev. **93**, 632 (1954).

[27]T. S. Moss, Proc. Phys. Soc. London, Sect. B **76**, 775 (1954).

[28]R. E. Peale, J. T. McWhirter, K. Muro, and A. J. Sievers, Solid State Commun. **60**, 753 (1986).

[29]S. P. Love, K. Muro, R. E. Peale, A. J. Sievers, and W. Lo, Phys. Rev. B **36**, 2950 (1987).